Astron. Astrophys. 330, 631–640 (1998)

ASTRONOMY
AND
ASTROPHYSICS

Long-term photometry of Be stars

III. Evidence for periodic outbursts of λ Eri and photometric activity in HR 2142⋆ ⋆⋆

R.E. Mennickent[1], **C. Sterken**[2,⋆⋆], **and N. Vogt**[3,4]

[1] Departamento de Física, Facultad de Ciencias Físicas y Matemáticas, Universidad de Concepción, Casilla 4009, Concepción, Chile (rmennick@phys.cfm.udec.cl)
[2] University of Brussels (VUB), Pleinlaan 2, B-1050 Brussels, Belgium (csterken@vub.ac.be)
[3] Grupo de Astrofísica, Universidad Católica de Chile, Casilla 314, Santiago, Chile
[4] Sternwarte Sonneberg, Sternwartenstr. 32, D-96515 Sonneberg, Germany (nikolaus.vogt@stw.tu-ilmenau.de)

Received 1 July 1997 / Accepted 15 September 1997

Abstract. Strömgren differential $uvby$ photometry of λ Eri and HR 2142 is analyzed. The data were taken during the time interval 1983–1994 in the framework of the Long-Term Photometry of Variables project at La Silla. λ Eri exhibited four photometric events (probably associated with line emission episodes) that last several months and which were characterized by a common pattern of change in all passbands ($\sim \pm 10^{-3}$ mag/day) along with an apparent decrease of the amplitude of the short-term variability and an increase of the stellar temperature. A search for periodicities reveals that these events fit a 486 d recurrence time. On the other hand, HR 2142 showed a relatively "quiet" long-term photometric behaviour, the orbital period being detected only marginally in the photometric data set. In contrast, a 344 d period optimally fits the data. We discuss the possibility of an internal "clock" regulating the outburst activity of λ Eri and show that the photometric variability of HR 2142 can hardly be explained by its interacting binary nature. We also discuss an empirical relationship found between $\frac{\partial c_1}{\partial u}$ and $v\ sini$ in a sample of 11 Be stars.

Key words: stars: emission-line, Be - stars: individual: λ Eri – HR 2142

1. Introduction

This is the third paper in a series which deals with differential *uvby* photometry of Be stars. The data were obtained at ESO in the framework of the "Long-term Photometry of Variables" (LTPV) project which was initiated more than a decade ago (Sterken 1983, 1994). In Paper I (Mennickent et al. 1994) we reported dramatic long-term variations on time scales of years for 7 Be stars, in Paper II (Sterken et al. 1996) we discussed 4 more stars with a relatively stable level of long-term brightness but with periodic or random fluctuations on shorter time scales. In the present paper we discuss two stars that show an almost constant long-term photometric level with additional, apparently-random, fluctuations.

2. Observations

Each star was, as a rule, observed together with two comparison stars. Table 1 gives the most important data for each star, as well as the overall averages in $y(V)$, $b-y$, m_1 and c_1, together with the corresponding standard deviations of individual measurements. The data in Table 1 are based on data from "System 7" (see Sterken et al. 1993) only, and they give a general impression of the photometric accuracy of the LTPV program. A quick look reveals first hints on the variability: in all cases the standard deviations of the program stars exceed those of the comparison stars—the fact that most program stars are slightly brighter than their comparison stars is of no influence on the mean errors, since at such bright apparent magnitudes the accuracy is not shot-noise dominated.

Throughout this paper we discuss differential photometry, for more details see also Paper I, in the sense that the variability of each program star P is discussed in terms of the differential magnitude of P *minus* the average of the corresponding signal for comparison star A and B in each Strömgren band.

For all differential Be star data a period search was carried out using two complementary methods: the "pdm" algorithm which is incorporated in the IRAF reduction program (Stellingwerf 1978) and the Analysis of Variance periodogram (Schwarzenberg-Czerny 1989) which is included in the MIDAS software. The second method has the advantage that the proba-

Send offprint requests to: R.E. Mennickent
⋆ Based on observations obtained at ESO, Chile
⋆⋆ Belgium Fund for Scientific Research (FWO)

Table 1. Program Be Stars (P) and Comparison Stars (A,B): average $y(\equiv V), b-y, m_1, c_1$ magnitudes and their standard deviations σ (in millimagnitudes). N denotes the total number of observations of each program star. Note that the results are based solely on data belonging to System 7 (Sterken et al. 1993, see also Sterken 1993)

HR	$y(V)$	$b-y$	m_1	c_1	N	σ_y	σ_{b-y}	σ_{m_1}	σ_{c_1}
HR 1671(A)	5.828	-0.033	0.113	0.649	203	7	4	6	6
HR 1617(B)	4.803	-0.081	0.098	0.241	223	8	5	6	6
HR 1679(P)	4.273	-0.069	0.062	0.049	233	40	46	42	56
HR 2205(A)	5.063	-0.086	0.091	0.206	173	9	5	6	6
HR 2344(B)	5.060	-0.079	0.095	0.216	174	8	5	6	5
HR 2142(P)	5.268	0.029	0.026	-0.013	175	14	4	6	10

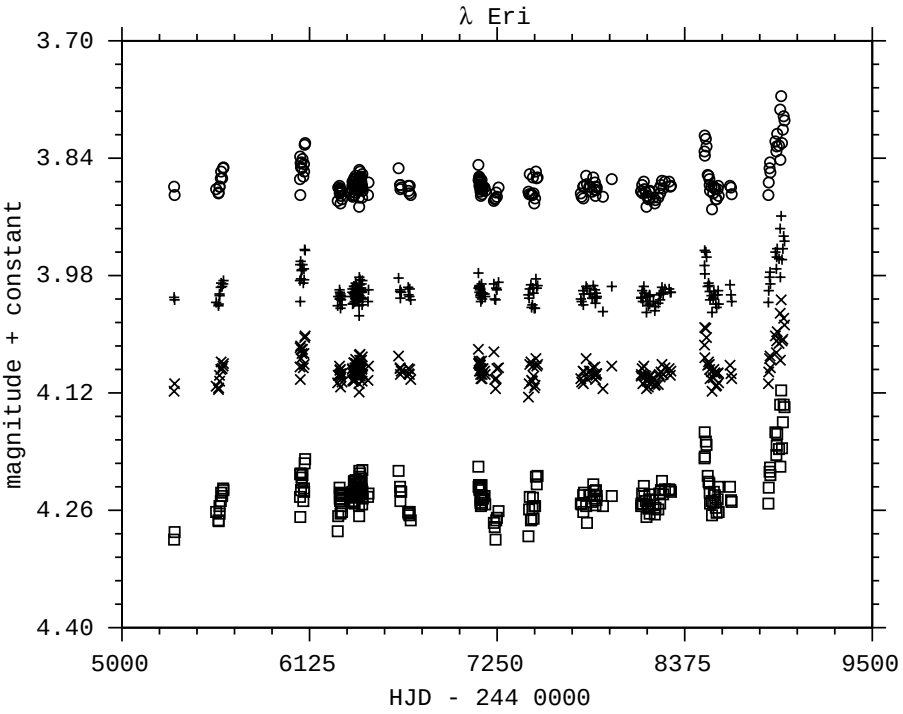

Fig. 1. Overall light curve of λ Eri. The $uvby$ magnitudes are shown as $\square$ $\times$ + and $\circ$, respectively. vby are shifted by $-0\overset{\mathrm{m}}{.}1$, $-0\overset{\mathrm{m}}{.}2$ and $-0\overset{\mathrm{m}}{.}4$, respectively.

bility distribution is known inclusive for small data samples and provides a robust significance criterion.

Part of the photometric data were published by Manfroid et al. (1991), Sterken et al. (1993), Manfroid et al. (1994) and Sterken et al. (1995), see also ESO Scientific Reports Nos 8, 12, 14 and 16, and we refer to these references for more details on the observing strategy and on the reduction procedure.

3. Results

3.1. λ Eri = HD 33328 = HR 1679

This star is characterized by a stable $0^{\mathrm{d}}702$ spectroscopic and photometric periodicity with a rapidly variable light amplitude from $0\overset{\mathrm{m}}{.}01$ to $0\overset{\mathrm{m}}{.}08$ in b (see, e.g., Bolton & Stefl 1990, Percy 1986, Balona 1990). An 8 h spectroscopic period has also been reported (Penrod 1986a, Smith 1989). Based on extensive radial velocity studies, Bolton (1982) and Smith (1989) did not find any evidence for binarity in this star. The short-term periodicities have been interpreted as evidence for non-radial pulsations and/or rotation of star spots. However, Balona (1995) has given solid arguments against these hypotheses for Be stars in general, showing the incompatibility between the models and the observed radial velocity to light amplitude ratio.

3.1.1. A search for periodicities

Our data do not show large photometric variability on time scales of years, but minor variability on time scales of weeks in all passbands is present (Fig. 1). However, a close examination of the u light curve reveals a smooth long-term oscillation with minima at HJD 244 5315 and 244 7241, 244 7438, yielding a quasi-period of 5.5 years. This oscillation seems to be almost

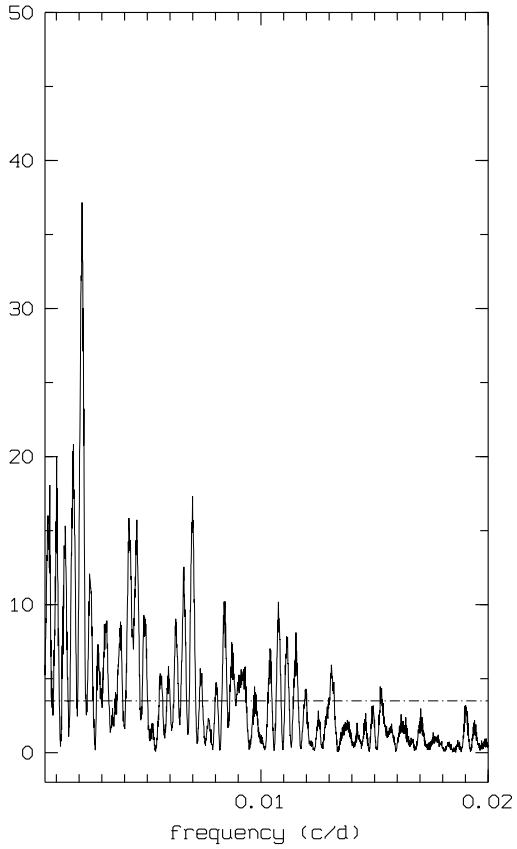

Fig. 2. λ Eri y data AOV periodogram. The 99% confidence level is shown by the dash-dot line.

completely masked by short-term variability at longer wavelengths. The above three minima also fit a 192.8(2) d period.

We searched for periodicities in the 1–1000 d range using the pdm and AOV statistics. Theoretically, the AOV statistics is 1 for pure noise, for uncorrelated observations and n_c for correlated observations, where n_c is the average number of correlated observations (Schwarzenberg-Czerny 1989). The periodogram divided by its expected value has Fisher-Snedecor probability distribution $F(r-1, n/n_c - 1)$ where r is the number of phase bins employed and n the number of datapoints. In our case, we have 232 points and choose 5 phase bins for adequately mapping the samples, so the 99% confidence level around the main peak is around $\frac{7}{2}$.

The periodograms revealed a strong peak at $f = 2.13(4)10^{-3}$ cycles/day, the error being calculated as the half width at the height of the line peak minus the mean noise level of the periodogram (Schwarzenberg-Czerny 1991 and Fig. 2). Significant power is also observed at the first subharmonic $f/2$. Both peaks are above the 99% confidence level.

When folding the light curves with the above periods, the phase curves are dominated by one and two wide "humps" (Fig. 3). The ephemeris relative to the main hump maximum are:

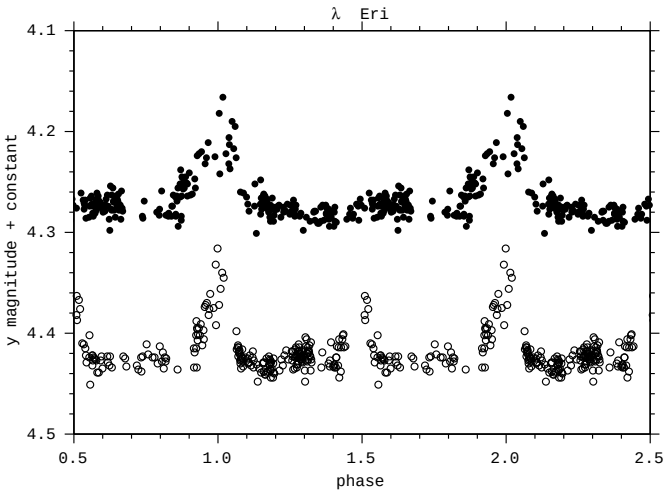

Fig. 3. y magnitudes phased with the 469 d (•) and 939 d (○) periods according to the ephemeris given by Eqs. (1) and (2). The latter have been shifted by $0^m.15$.

$$HJD(max) = 244\,5660(75) + 470(9)\,E \quad (1)$$

$$HJD(max) = 244\,6139(122) + 939(9)\,E \quad (2)$$

A close examination of these humps reveals that they are the combined effect of several *rising-fading* events occurring in different epochs. In the following, we pass to analyze in detail these events.

3.1.2. "Fading-rising" and "flare-like" events

In general, the medium-term variability of λ Eri (time scale of weeks to months) can be described as epochs of certainly random variability (eg. around HJD 244 6440 and between HJD 244 7760 – 244 8290) and epochs of rise or decline which we have called "rising-fading events". We have identified four such events in our data sample (Fig. 4):

– *Event at HJD 244 5578:* This minor brightness change lasts 30 days and is characterized by a brightening in all bands at a very similar rate, the color indices remaining practically unchanged. Two spectra taken at the beginning of our observations (HJD 244 5571 and 244 5586) did not reveal emission at Hα (Penrod 1986b), however double-peaked emission appeared 35 days after our last observation. The brightness event here reported could be the precursor of the mass ejection event reported by Penrod.

– *Event at HJD 244 7137:* This 23 day fading did also not show significant color changes. After an observational gap of 52 days the star appears still fading, reaching a minimum in u on HJD 244 7240 (Fig. 5). The next season the star was found at the beginning of a rising in the u band at HJD 244 7438. This event was spectroscopically monitored by Smith et al. (1991) who studied the kinematics of

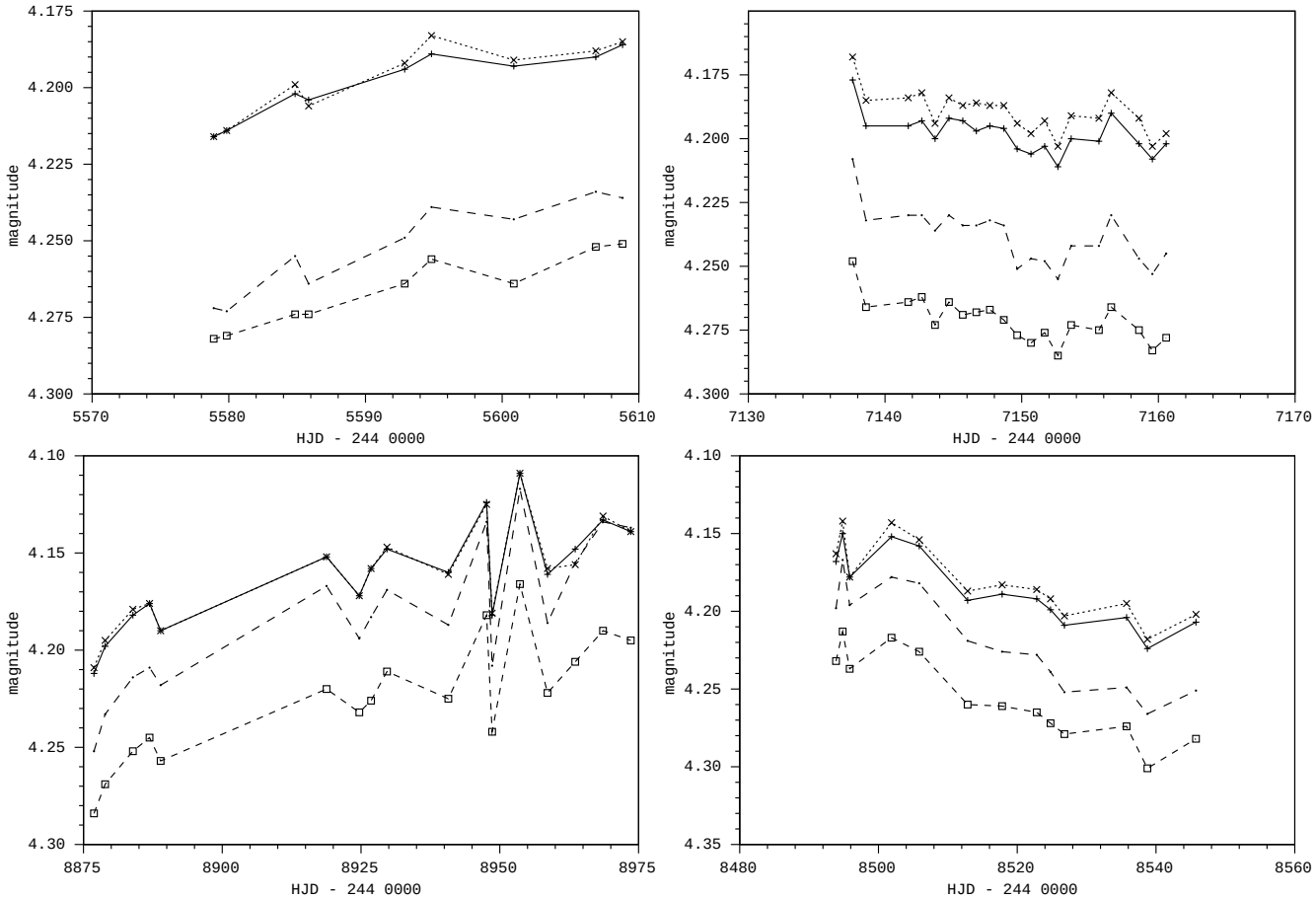

Fig. 4. Fading-rising events of λ Eri. $uvby$ magnitudes are shown as □ + × and · respectively.

the circumstellar material using the Hα, He I λ 6678 and C II λ 6578–6583 lines (Smith et al. 1991). On the assumption that the evolution is caused by a slow expansion of a detached, thin, quasi-Keplerian ring, the peak separation suggests a ring radius increasing from 5.8 to 9.6 stellar radii over 5 months. In Fig. 5 we have plotted the Hα peak separation as reported by these authors, versus the photometric u and v magnitudes. It is evident that the disk formation was accompanied by a fading in brightness, the star being probably obscured by increasing amounts of circumstellar matter.

The oscillation starting around HJD 244 7450 coincides with the appearance of a strong redshifted emission peak detected at Hα on HJD 244 7449 by Smith et al. (1991). These authors explained this spectroscopic feature as due to a continuos "rain" of low-angular momentum material falling into the star's surface with maximum velocities of the order of 250 km s^{-1}. Based on a measured profile's broadening of 130 km s^{-1}, they estimated a maximum surface heating $\sim 10^6$ K. Smith et al. (1991) argued that turbulence may diffuse the energy into the deeper layers and moderate the heating, producing thermal signatures of self-accretion at far-UV and/or soft X-ray wavelengths, a spectral domain far out of the range of our photometry.

– *Event HJD at 244 8493:* This fading lasts 52 days and was accompanied by an increase of the c_1 index by $\approx 0\overset{\mathrm{m}}{.}02$, while the $b-y$ and m_1 index were slightly bluer and redder, respectively. The steepest gradient was observed in the u band.

– *Event HJD at 244 8877:* This long-lasting brightness (97 days) was accompanied by a fading of the c_1 color index by $0\overset{\mathrm{m}}{.}05$ and a smooth increase of the $b-y$ color while m_1 remained almost constant. Sharp brightening episodes occurred on HJD 244 8947.6, HJD 244 8953.6 and HJD 244 8968.6. The u band was the most influenced, fading by $0\overset{\mathrm{m}}{.}07$ in less than 5.0 days. During these maxima the star reached its maximum luminosity during the 1983–1992 interval (u = 4.117, y = 4.166) with a flat uvb spectrum.

3.1.3. General properties of rising-fading events

For every event we measured duration, amplitude and the coefficient β_i defined by:

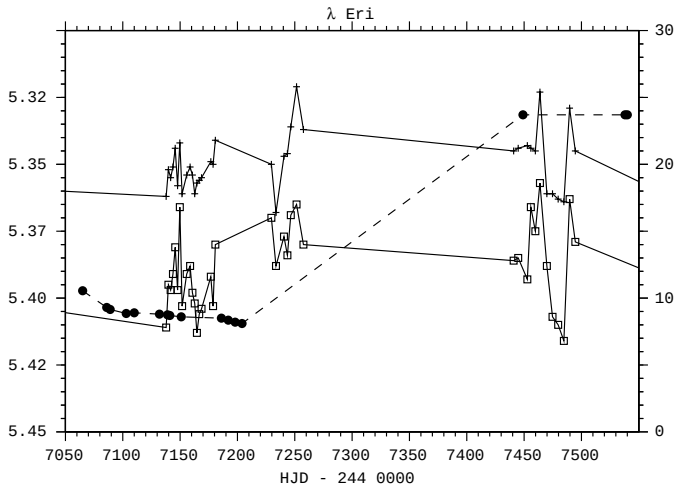

Fig. 5. The events following the fading event on HJD 244 7137. The figure shows u (□) and v (+) magnitudes (left scale) together with the Hα peak separation (•, in Å, right scale) as derived from Fig. 5 of Smith et al. (1991).

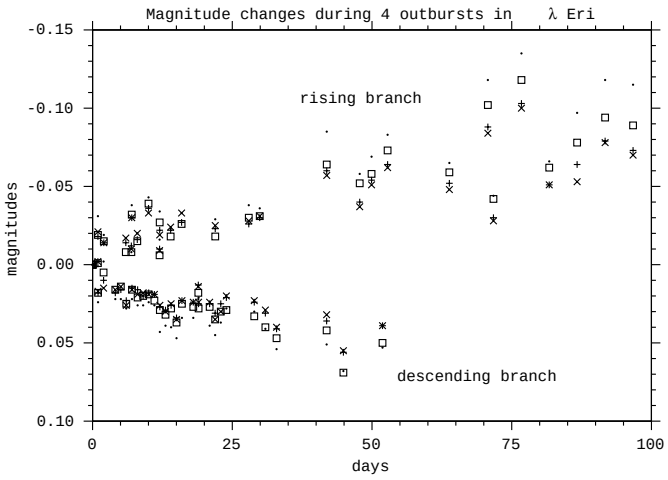

Fig. 6. General pattern of rising-fading events in λ Eri. Symbols are as in Fig. 2. Data of 4 events have been combined in the following way: the vertical scale refers to differential magnitudes calculated as Δm = $m - m(t_0)$, where $m = u, v, b, y$ and t_0 the time at the beginning of every event. The horizontal axis shows time defined as $t - t_0$. The events seems to be characterized by a similar slope.

$$m = \alpha_i + \beta_i(\text{HJD} - 244\,0000) \quad i = u, v, b, y \tag{3}$$

The results are shown in Table 2. We observed that a similar pattern holds for the four events covered by the LTPV data. This is easily seen in Fig. 6 which compares slopes of risings and fadings for different filters. In average, the star rises at a rate $-0.88(1)10^{-3}$ mag/day and declines with $1.1(1)\ 10^{-3}$ mag/day, though small but significant differences among events and filters are observed. A remarkable fact is the low rms value obtained in each fit, which is well below the reported amplitude of short-term variations. Such low rms values during long observing runs probably reflect a fading of the short-term variability amplitudes during rising-fading events, at least in the four reported cases. Another remarkable fact is the anticorrelation found between the c_1 and $b-y$ index during the higher amplitude events (at HJD 244 7137 and HJD 244 8877).

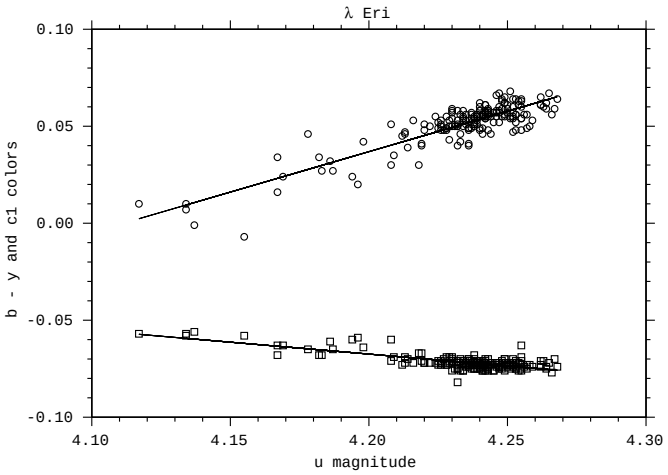

Fig. 7. The $b-y$ (□) and c_1 (○) colors correlated with the u magnitude. Only data in one homogeneous photometric system (System 7) have been considered. Best linear fits given by Eqs. (4) are shown.

3.1.4. Color changes

As pointed out by Sterken et al. (1996), systematic differences exist between different photometric systems used during the LTPV project. These differences were virtually absent in v, b and y, and minor but commensurable in u. So, color changes, specially c_1 variations, must be discussed considering one homogeneous photometric system. We selected System 7 (corresponding to data obtained with the Strömgren Automatic Telescope [SAT]), in which the bulk of the LTPV observations were made.

Color changes exhibited by λ Eri are similar to those found in other Be stars (e.g. Mennickent et al. 1994). We can express the observed correlations between $b-y$, c_1 and u as (Fig. 7):

$$b - y = -0.12(1)\,u + 0.45(3) \tag{4.1}$$

$$c_1 = +0.45(3)\,u - 1.71(7) \tag{4.2}$$

3.2. Temperature changes

The reported absence and/or weakness of Hα emission in λ Eri during the past, supports the hypothesis that the circumstellar reddening is small except during outburst. Therefore we may apply the calibrations of photometric parameters derived for normal non-emission B type stars — though keeping in mind that the accuracy of our results is compromised by a possible

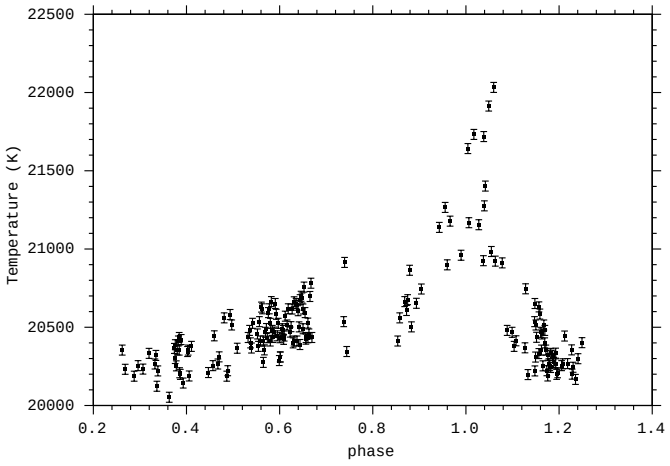

Fig. 8. Phase-Temperature diagram for λ Eri accordingly to ephemeris given by Eq. (1).

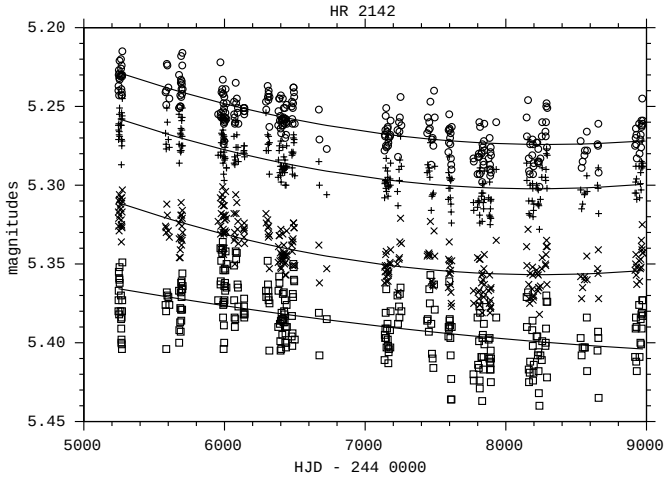

Fig. 9. Overall light curve of HR 2142. The $uvby$ magnitudes are shown as □ × + and ○, respectively. Long-term tendencies are indicated by parabolic fits.

small and variable circumstellar reddening and high rotation. The $u-b$ color is a most sensitive ground-based photometric indicator of temperature variations for early B-type stars. We derived the effective temperature using the $[u-b]$-based calibration of Napiwotzki et al. (1993), where $[u-b]$ is the $u-b$ index corrected for interstellar reddening. The mean temperature, excluding outbursts (i.e. data in phases [0.92-0.08]), is 24 000 K, with a standard deviation of 450 K. It implies a spectral type of B 1.5(5) accordingly to the spectral type vs. $T_{\rm eff}$ calibration derived from Table 1 of Popper (1980). The above temperature is slightly higher than the one derived by Theodossiou (1985) by fitting computed to observed fluxes in the visible and ultraviolet spectral range ($T_{\rm eff}$ = 22 500K). The temperature's accuracy can be estimated from the $u-b$ scatter exhibited by the check star HR 1671, which has a standard deviation of $0\overset{\rm m}{.}003$ that yields a temperature uncertainty of ~ 40 K. On the other hand, its inferred temperature is 12 672, which implies a spectral type B 6.9(5), accordingly to the Popper (1980) calibration, a figure close to the reported B8 spectral type (e.g. Sterken et al. 1995). The phase-temperature diagram for λ Eri is shown in Fig. 8. Due to an unknown component of circumstellar reddening during outburst, the datapoints around maximum really represent low limits to the photospheric temperature. A notable fact is the secular temperature increase, from 20 200 → 20 600 K prior to outburst. This could be interpreted as an input of thermal energy in the photosphere prior to the formation and ejection of an envelope.

3.3. HD 41335 = HR 2142

This star is an interacting binary with an orbital period P_{orb} = $80\overset{\rm d}{.}860$ (Peters 1983). The long-term photometric behaviour is characterized by a smooth fading in all passbands reaching a minimum around HJD 244 8000 and a subsequent reversing tendency (Fig. 9). The overall change in magnitude through this cycle is very small, amounting to $0\overset{\rm m}{.}05$ at y and slightly lower amplitudes in other bands. This behaviour coincides with an almost constant Hα emission strength during 1982–1993 (Hanuschik et al. 1996). Mild random photometric variability (amplitudes $\sim 0\overset{\rm m}{.}08$ at u) is observed on time scales of weeks. Colors are almost constant. When searching in the 0.1–1000 d interval, periods at 392, 344, 151 and 103 d appeared persistently in the pdm θ window for all passbands along with other less significant peaks. After removing the long-term tendency by subtracting a parabolic or linear least squares fit to the data, the corresponding periodograms looked noisier and the above peaks tended to dissappear. In order to check this result and to investigate the statistical significance of the above periods, we also applied the AOV method to the original data. The periodograms looked very similar at different passbands, an example is shown in Fig. 10.

As we see, several frequencies have significancies greater than 99%. The most prominent peaks occurs at 2.91(2) 10^{-3}, 2.55(4) 10^{-3}, 9.66(4) 10^{-3} and 6.62(6) 10^{-3} cycles/day. The frequency corresponding to the orbital period (1.237 10^{-2} cycles/day) appears as a minor but significant peak in the periodogram. However, their influence in the power spectrum could be surprisingly significant. In fact, the 103 and 151 d periods could correspond to the 1 and 2 cycles/year aliases of the orbital period, whereas the two longer periods can be interpreted as a beat between 81 d and a period close to their 1 c/yr alias. The strange fact is the very high power exhibited by these secondary frequencies, specially the two longer.

We have folded the data with the above periods and also with the orbital period using the zero point given by Peters (1983), viz. T_0 = 244 1990.5, and fit the resulting phase diagrams with sinusoids:

$$m_i = m_{i,0} + A_i cos(2\pi \tfrac{t-T_0}{P}) + B_i sin(2\pi \tfrac{t-T_0}{P}) \qquad (5)$$

The results are shown in Table 3. The best fit, characterized by a minimum of the σ/K ratio (where σ and K are the fit's dispersion and semi-amplitude, respectively), occurs when fold-

Table 2. Fading-rising events in λ Eri. We give the (HJD - 244 000) of our first observation, the duration of the ascending or descending branch (in days) and their amplitude A (in tenths of magnitude) in every band-pass, the linear gradient β_i ($\times 10^{-4}$ mag/day). We also give the regression coefficient ρ and the rms (in milimagnitudes) of the fits defined by Eq. 1.

HJD	Δt	u				v				b				y			
		β_u	ρ	rms	A	β_v	ρ	rms	A	β_b	ρ	rms	A	β_y	ρ	rms	A
5578	30	-13(2)	0.9	5	4	-10(2)	0.8	6	4	-9(1)	0.9	4	3	-10(1)	0.9	4	3
7137	23	11(3)	0.7	8	5	8(2)	0.6	6	4	7(2)	0.6	6	3	9(2)	0.7	6	4
8493	52	17(2)	0.9	13	10	11(2)	0.8	13	8	12(2)	0.9	11	7	14(2)	0.9	11	9
8877	97	-9(2)	0.8	22	14	-6(1)	0.8	17	10	-6(1)	0.8	17	10	-8(1)	0.8	18	12

Table 3. Parameters of the fits given by Eq. (5). For every frequency (f, times 10^{-3} cycles/day), the half amplitudes (K) and dispersions (σ) are also given.

f	Filter	m_0	A	B	K	σ
12.37	u	5.387(1)	0.0021(18)	0.0056(18)	0.0060(23)	0.0208
	v	5.344(1)	0.0009(15)	0.0091(15)	0.0092(16)	0.0175
	b	5.290(1)	0.0015(15)	0.0077(14)	0.0079(17)	0.0169
	y	5.261(1)	0.0027(15)	0.0074(15)	0.0079(19)	0.0172
9.66	u	5.389(1)	0.0055(17)	0.0102(18)	0.0116(23)	0.0197
	v	5.345(1)	0.0057(14)	0.0117(15)	0.0130(19)	0.0165
	b	5.291(1)	0.0061(13)	0.0106(14)	0.0122(19)	0.0157
	y	5.262(1)	0.0066(14)	0.0100(14)	0.0120(20)	0.0161
6.62	u	5.387(1)	0.0039(18)	0.0058(18)	0.0070(25)	0.0200
	v	5.343(1)	0.0059(15)	0.0077(15)	0.0097(21)	0.0170
	b	5.289(1)	0.0062(14)	0.0071(14)	0.0094(20)	0.0160
	y	5.260(1)	0.0066(14)	0.0066(14)	0.0093(20)	0.0160
2.91	u	5.385(1)	0.0114(17)	0.0086(15)	0.0143(23)	0.0186
	v	5.340(1)	0.0112(13)	0.0125(12)	0.0168(18)	0.0144
	b	5.286(1)	0.0106(12)	0.0114(12)	0.0156(17)	0.0139
	y	5.258(1)	0.0104(13)	0.0114(12)	0.0154(17)	0.0143
2.55	u	5.389(1)	-0.0092(17)	0.0068(18)	0.0115(24)	0.0193
	v	5.344(1)	-0.0094(14)	0.0084(15)	0.0126(20)	0.0160
	b	5.290(1)	-0.0870(13)	0.0087(14)	0.0123(19)	0.0150
	y	5.261(1)	-0.0098(13)	0.0092(14)	0.0134(19)	0.0148

ing the data with the 344 days period (Fig. 11). We also show in Figs. 12 and 13 the phase diagrams for the periods 103 d and 81 d. The 392 d period yields to a phase diagram with extremely large data gaps.

As HR 2142 is a interacting binary consisting of an emitting disk, we can explore some other scenarios in order to explain their photometric variability. We can think about the 344 d periodicity as due to changing aspects of an ellipsoidal precessing envelope. In fact, both two-dimensional hydrodynamical simulations as well as numerical calculations (e.g. Whitehurst 1988, Hirose & Osaki 1990, Whitehurst & King 1991) indicate that a disk immersed in the Roche Lobe of the primary of a binary system should precess with a period (P_{pr}) related to the system's mass ratio ($q = M_2/M_1$) and orbital period:

$$\frac{P_{pr}}{P_o} \approx \frac{3.85(1+q)}{q} \qquad 0.1 \leq q \leq 0.22 \qquad (6)$$

In the case of HR 2142, $q \approx 0.09$ (Peters 1983) and the predicted $P_{pr} \approx 3770\overset{\mathrm{d}}{.}3$ is too long when compared with the observed long-term photometric periodicities. On the other hand, the beat period between the orbital and precession period is 79 d and 83 d depending on the prograde-retrograde nature of the precession. We see that the observed periodicities cannot be explained by changing aspects of an ellipsoidal precessing envelope neither by the orbital motion of the hot spot.

On the other hand, when folding the light curve with the orbital period, we obtain a very smooth sinusoidal curve with maximum at phase 0.08(1) which is compatible with the hypothesis of weak mass transfer in the binary system. In fact, such light curves are commonly observed in semi-detached binary systems like dwarf novae, being interpreted as due to the passage of a hot disk region (the so called "hot spot") along the observer line of sight. This hot spot is believed to be produced by the impact of the gas stream with the accretion disc. This picture is strongly supported by the periodic shell phases detected in the optical spectra (e.g. Peters, 1983). However, the amplitude of the "humps" seen in dwarf novae increase with the system inclination angle, being larger in equator-on systems. In contrast, the amplitude in HR 2142 (seen about 15^o out of the plane of the orbit, Peters 1983) is $\sim 0\overset{\mathrm{m}}{.}01$. This means the hot spot should contribute between 1.2 and 1.6% to the total continuum luminosity.

The hot spot can also be evidenced from the changing asymmetry of the double emission profiles. This asymmetry

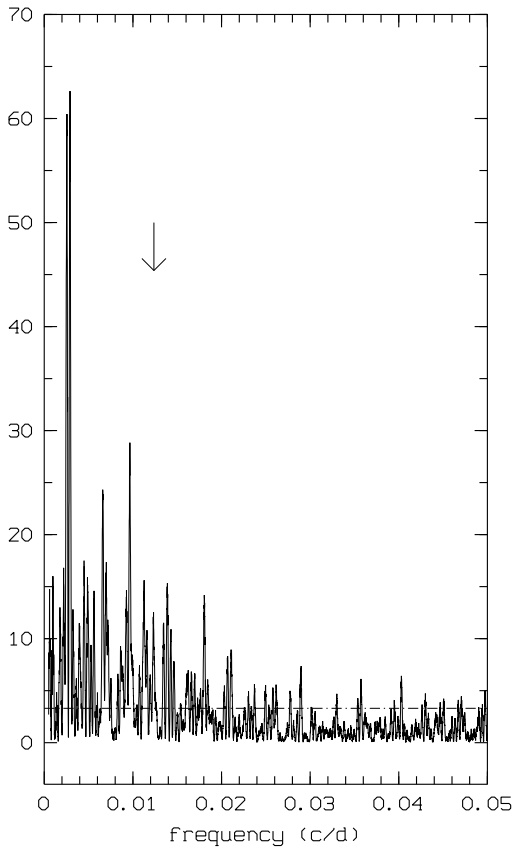

Fig. 10. The AOV periodogram for y data of HR 2142. The 99% confidence levels are indicated by dash-dot lines. The orbital frequency (0.01237 c/d) is indicated by an arrow.

is often measured as the ratio V/R between the intensities of the violet and red peaks referred to the continuum level (i.e. $V/R = (I_v - I_c)/(I_r - I_c)$). From the amplitude of V/R variations exhibited by the Hα emission lines given by Hanuschik et al. (1996) we deduced a contribution of the hot spot to the disk *line* luminosity of 30%. This contribution is $\sim 20 - 25$ times larger than the contribution to the *continuum* luminosity. This difference can be explained as due to different mechanisms producing the line and continuum radiation. In fact, whereas the continuum is mainly produced by the Be star flux, with little contribution of the secondary and envelope, the line emission is probably produced in the envelope by ionization and subsequent "cascade" recombination.

The hot spot luminosity is given by (e.g. Warner 1995, p. 83):

$$L_{sp} = \frac{f}{8}\frac{GM_1\dot{M}}{r_d} \quad (7)$$

where M_1, r_d and $\dot{M}$ are the primary mass, outer disc radius and mass transfer rate, respectively and f an efficiency factor ~ 1. Adopting values given by Peters (1983), viz. $M_1 = 11M_\odot$, $r_d = 20R_\odot$ and $\dot{M} > 10^{-8}M_\odot/yr$, we get $L_{sp} > 8.3\ 10^{31}$ erg s^{-1}. This luminosity is extremely low when compared with

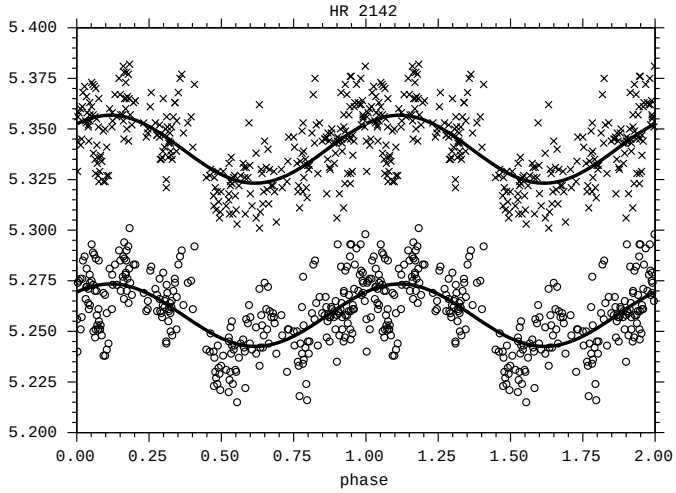

Fig. 11. The v (top), y (bottom) light curves folded with the 344 d period. Best sinusoid fits (Eq. 4) are shown.

the expected luminosity of a B2 IV star ($\sim 5\ 10^{35}$ erg s^{-1}). Therefore, if the hot spot luminosity were due to accretion, a mass loss rate $\sim 10^{-7}M\odot/yr$ should be needed for contributing 1% to the continuum flux as observed. This is a rather high value when compared with typical mass loss rates (at the envelope, due to inflow or outflow but not necessarily requiring a donor secondary star) deduced from the IR excess observed in Be stars.

3.3.1. Color changes

The overall color changes exhibited by HR 2142 are similar to those found in other Be stars (e.g. Mennickent et al. 1994). We can express the observed correlations as (Fig. 14):

$$b - y = -0.02(1)\,u + 0.16(6) \quad (8.1)$$

$$c_1 = +0.53(3)\,u - 2.89(23) \quad (8.2)$$

These correlations will be discussed in the next section.

4. Discussion

4.1. Periodic outbursts of λ Eri

For the first time we have a general picture of the outburst activity of λ Eri. The outbursts, probably linked to line emission episodes, last several months and have been only partially covered in the past mainly due to short campaigns lasting only few weeks. The outbursts follow an almost "universal" pattern of rising-falling which probably reflects the formation and dissipation of a circumstellar envelope. The decrease of the photometric dispersion around the main light curve during such episodes probably reflects a damping and/or occultation of the photospheric activity during the ejection process. More surprising yet, is the apparent periodicity followed by these outbursts and the probable heating of the photosphere prior to outburst.

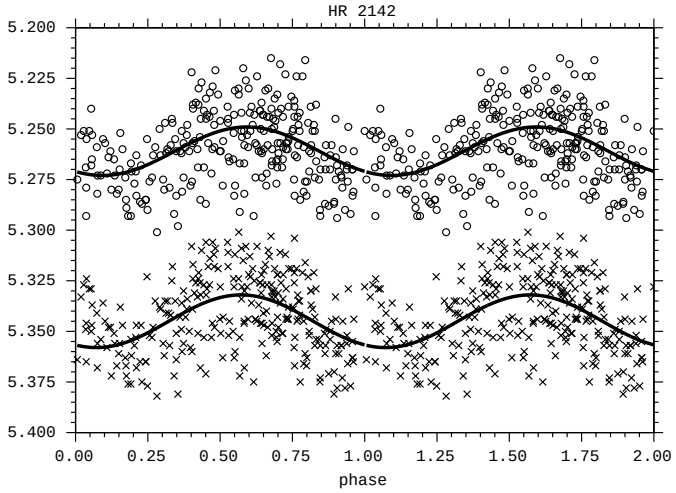

Fig. 12. The v (top), y (bottom) light curves folded with the 103 d period. Best sinusoid fits (Eq. 4) are shown.

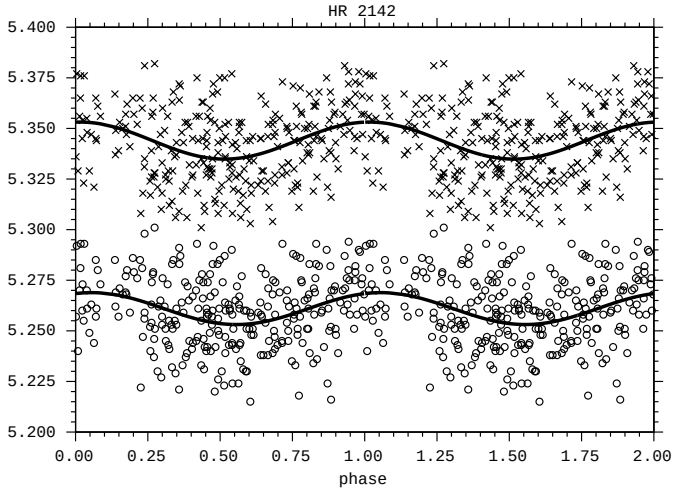

Fig. 13. The v (top), y (bottom) light curves folded with the orbital 80.86 d period accordingly to the ephemeris given by Peters (1983). Best sinusoid fits (Eq. 4) are shown.

As the star is probably not a binary (e.g. Smith 1989), a "stellar clock" is probably responsible for the periodicity. The existence of such a clock must be tested by future observations, and if proved, should be a clear indication for a periodic internal mechanism regulating the outburst activity of Be stars. Recently, Rivinius et al. (1997) suggested that the outbursts of the bright Be star μ Cen do not occur at random but follow a coherent temporal pattern. Due to poor spectroscopic coverage, it is not clear if this is also the rule for Be stars.

4.2. HR 2142: photometric variations probably not due to mass transfer

The most significant period is found at 344 d, which cannot be easily associated to the star's binarity, especially due to its high power when compared with the power of the orbital period. The

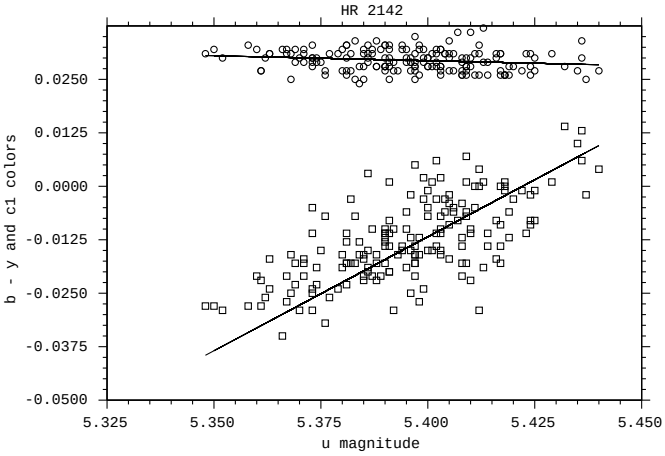

Fig. 14. The $b-y$ (□) and c_1 (○) colors correlated with the u magnitude. Only data in one homogeneous photometric system (System 7) have been considered. Best linear fits given by Eqs. (8) are shown.

only way is through a constructive (not random) interference between 81 d and their 1 c/yr alias. The weak photometric signal found at the orbital frequency along with the high mass transfer rate needed to produce it ($\sim 10^{-7} M \odot /yr$), suggest that another phenomenon rather than mass transfer, is modulating the radiative flux of HR 2142.

4.3. The $\beta_c - v\ sini$ relationship in Be stars

As already discussed in paper I each variable Be star seems to be characterized by a linear relationship between the u magnitude and the c_1 index in the sense:

$$u = \alpha_c + \beta_c c_1 \tag{9}$$

A linear least squares fit reveals for each star a coefficient β_c , i.e. the rate of change of the c_1 index with respect to the u magnitude. Table 4 lists the resulting coefficients β_c for all (except 2) stars of our sample in papers I, II and the present paper III, together with the corresponding $v\ sin\ i$ values. The two omitted stars are HR 3237 (paper I) which has a rather peculiar, non-linear relationship between c_1 and u, and HD 173219 (paper II) whose $v\ sin\ i$ value is not available.

9 of the 11 stars in Table 4 obey a well defined linear relationship between β_c and $v\ sin\ i$:

$$\beta_c = 0.23(5) + 0.00092(19) v\ sin\ i \tag{10}$$

with standard deviation 0.06 and correlation coefficient 0.87. Only two stars were excluded in fit (10), V 923 Aql and HR 2855, whose β_c values are placed far outside the range defined by the remaining stars. This could have simple reasons: V 923 Aql is much cooler than all other Be stars, its spectral type B6 deviates considerably from the range B0–B3 of the remaining sample stars. Just the opposite is valid for HR 2855 which is the only case of negative c_1 values, probably due to

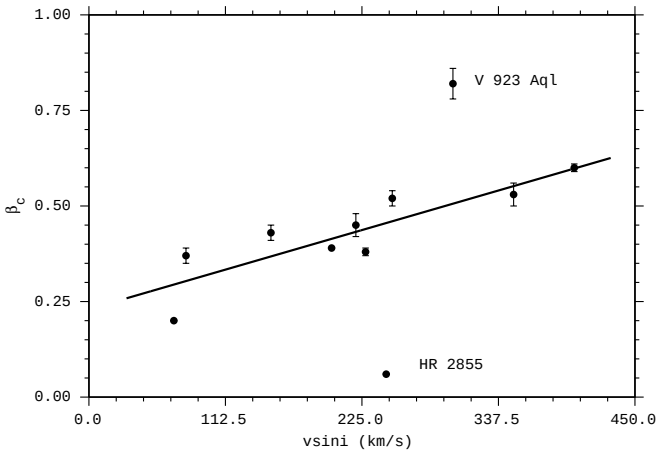

Fig. 15. The $\beta_c - v\ sini$ relationship in Be stars. The best linear fit excluding V 923 Aql and HR 2855 is shown. Data are from Table 4.

Table 4. The rate of change of c_1 with respect to u for the sample of Be stars analyzed in Papers I, II[†] and III[‡].

HD	$v\ sini$	β_c
33328[‡]	220	0.45(3)
41335[‡]	350	0.53(3)
48917[†]	200	0.39
56014	150	0.43(2)
56139	80	0.37(2)
58978[†]	245	0.06
89890[†]	70	0.20
142983	400	0.60(1)
183656	300	0.82(4)
184279	228	0.38(1)
205637	250	0.52(2)

an abnormally strong UV excess. We can tentatively conclude that relationship (10) seems to be valid in the range $0 < c_1 < 0.7$, i.e. for the hotter Be stars without strong UV excess. The strength of the Balmer jump reacts on brightness variations in the u band more sensitively for large $v\ sin\ i$ Be stars, i.e. in stars seen preferentially under large inclinations.

Acknowledgements. We thank the referee, Dr. J. Percy, for useful suggestions about a first version of this manuscript. Gratitude is expressed towards all observers of the LTPV project: without their help and dedication, a study of this extent would never have been possible. R.M. acknowledges the support of Dirección de Investigación de la Universidad de Concepcion, Chile, P.I.# 95.11.11.1-1, FFM 96-01 and FONDECYT 1971064. The authors are indebted to Dr. Dietrich Baade for his collaboration in the early stages of the Long-Term Photometry of Variables project, and especially for selecting the target stars and for supervising the first observations. This research has made use of the SIMBAD database, operated at CDS, Strasbourg, France. C.S. acknowledges financial support from the Belgian Fund for Scientific Research (NFWO).

References

Balona L.A., 1990, MNRAS 245, 92
Balona L.A., 1995, MNRAS 277, 154
Bolton C.T., 1982, in *IAU Symposium 98, Be Stars*, ed. M Jaschek and H.-G. Groth (Dordrecht, Reidel), p. 181
Bolton C.T., Stefl S., 1990, in *Mass Loss and Angular Momentum for Hot Stars*, ed. L.A. Wilson, and R. Stalio (Dordrecht, Kuwler), in press.
Hanuschik R.W., Hummel W., Sutorius E., Dietle O., Thimm G., 1996, A&AS 116, 309
Hirose M., Osaki Y., 1990, PASJ 42, 135
Manfroid J., Sterken C., Bruch A. et al., 1991, A&AS 87, 481
Manfroid J., Sterken C., Cunow B. et al., 1994, A&AS 109, 329
Mennickent R.E., Vogt N., Sterken C., 1994, A&AS 108, 237 (Paper I)
Napiwotzki R., Schönberner D., Wenske V., 1993, A&A 268, 653
Penrod G.D., 1986a, in *IAU Colloquium 92, The Physics of Be Stars*, ed. A. Slettebak, and T. Snow (Cambridge, Cambridge University Press), p. 463
Penrod G.D., 1986b, PASP 98, 35
Percy 1986, PASP 98, 342
Peters G., 1983, PASP 95, 311
Popper D.M., 1980, ARA&A 18, 115
Rivinius T., Stefl S., Baade D., Stahl O, Wolf B., Kaufer A., 1997, submitted to Be star newsletter.
Schwarzenberg-Czerny A., 1989, MNRAS 241, 153
Schwarzenberg-Czerny A., 1991, MNRAS 253, 198
Smith M.A., 1989, ApJS 71, 357
Smith M.A., Peters G.J., Grady C.A., 1991, ApJ 367, 302.
Stellingwerf R.F., 1978, ApJ 224, 953
Sterken C., 1983. *The Messenger* 33, 10
Sterken C., 1994, in *The Impact of Long-Term Monitoring on Variable-Star*
Sterken C., 1993, in *Precision Photometry*, D. Kilkenny, E. Lastovica, J. Menzies (Eds.), South African Astronomical Observatory, 57
Sterken C., Manfroid J., Anton K., et al., 1993, A&AS 102, 79
Sterken C., Manfroid J., Beele D., et al., 1995, A&AS 113, 31
Sterken C., Mennickent R.E., Vogt N., 1996, A&A 311, 579 (Paper II)
Theodossiou E., 1985, MNRAS 214, 327
Warner B., 1995, in Cataclysmic Variable Stars, Cambridge University Press
Whitehurst R., 1988, MNRAS 232, 35
Whitehurst R., King A., 1991, MNRAS 249, 25

Note added in proof: G. Peters call my attention to the fact that the 486d recurrence time observed in λ Eri is very close to the 1.3 yr periodicity found by her in a study on tong-term wind activity in this star (BAAS, 25, 742, 1993). She independently found a Teff of 24,000 K from fitting Kurucz models to the IUE flux (Peters, G., in preparation). In addition, she noted that the 344d period found by us in HR 2142 is about 4 times the orbital period. This coincides with the observed cyclic changes in the strength of (Balmer) shell line recurring every 4–5 shell phases. She mentioned the possibility that enhanced mass transfer rate episode could be occurring due to an oscillation of a still undetected late-type secondary about its Roche surface that would lead to variations in the shell phases, which have been interpreted as absorption in the main gas stream and a counterstream that swing into our line-of-sight every binary orbit.

This article was processed by the author using Springer-Verlag LaTeX A&A style file *L-AA* version 3.